NANO LETTERS

pubs.acs.org/NanoLett

Photoreduction at a Distance: Facile, Nonlocal Photoreduction of Ag Ions in Solution by Plasmon-Mediated Photoemitted Electrons

Seung Joon Lee,[†] Brian D. Piorek,[‡] Carl D. Meinhart,[§] and Martin Moskovits*[,†]

[†]Department of Chemistry and Biochemistry , [‡]Institute for Collaborative Biotechnologies and California NanoSystems Institute and , [§]Department of Mechanical Engineering, , and University of California, Santa Barbara, California 93106

ABSTRACT Surface-immobilized, densely packed gold nanoparticles in contact with aqueous silver ions and exposed to red light rapidly photoreduce silver ions in solution producing radially symmetric metal deposits with diameters many times larger than the diameter of the illuminating laser beam. The average particle sizes in the deposit increase with radial distance from the center of the deposit. This reduction-at-a-distance effect arises from surface-plasmon-mediated photoemission, with the photoemitted electrons conducting along percolating silver pathways, reducing silver ions along these conducting channels and especially at their periphery, thereby propagating the effect of the illuminating laser outward.

KEYWORDS Surface-enhanced Raman, photoreduction, plasmonics

The field of plasmonics, which arose out of the discovery of surface-enhanced Raman spectroscopy (SERS), has spawned two robust paradigms: (i) that plasmonic nanostructures with appropriate architectures, constructed from appropriate materials and excited at the right wavelengths can concentrate light at specific nanosized locations leading to exotic optical effects,[1−4] and (ii) that plasmonic energy can be transmitted from the point of excitation to points many wavelengths away where it can carry out photochemical or photophysical processes.[5−7]

Here we show that a dense layer of surface-immobilized gold nanoparticles can massively photoreduce silver ions in a solution in contact with the nanoparticles, through two-photon-induced electron photoemission by red light, forming large symmetrical silver deposits with diameters many times that of the illuminating laser beam. We prove that the initiation of the photoreduction process is surface-plasmon (SP)-mediated electron photoemission from the metallic nanoparticles into the solution by measuring the sign and magnitude of the recharge current that partially replenishes the photoemitted electrons to a steady state. We propose that the large lateral size of the deposit arises from charge conduction of the photoemitted electrons along percolating silver deposits (perhaps also aided by plasmonic propagation) allowing the reduction of silver ions to take place at locations remote from the illuminated spot.

A schematic representation of the experiment is illustrated in Figure 1. Experiments were carried out on glass cover slides functionalized with (3-aminopropyl)triethoxysilane (APS) to help immobilize the Au nanoparticles (AuNPs) subsequently deposited onto the functionalized slide out of a gold colloid solution prepared by citrate reduction.[8,9] After NP decoration, samples were thoroughly washed with water and toluene to remove residual organic species. The surface-anchored AuNPs were functionalized with 4-mercaptobenzoic acid (MBA) as a SERS probe for monitoring the silver nanoparticle growth kinetics.

Scanning electron micrography (Figure 1, panels A−C) shows the structure of the silver deposits produced following irradiation by 632.8 nm laser light. The diameter of the beam is approximately 1 μm corresponding approximately to the small central area (~1.3 μm) visible in panels A and B of Figure 1. The deposits are clearly much larger than the diameter of the beam implying that the effect of irradiation propagates rather far from the point of illumination. The much smaller AuNPs are also visible as a dense carpet covering the entire slide. The uniformity of the AuNP coverage has also been disrupted by the silver growth and in places incorporated into the deposits.

The symmetry and mass distribution of the silver growth are intriguing. At low light doses (4.25 mW, 10 s) the growth shows a symmetrical flower-like pattern of connected particles, increasing uniformly in size as one proceeds outward from the center. The deposit, for the most part, consists of continuous, or at least percolating, metal. Also, the silver deposits formed after longer exposures to light seem to have primarily larger mass rather than larger overall radii (Figure 1A−C), possibly reflecting the characteristic range of the conduction process that allows the effect of the photoemission to operate at a distance. The preferential deposition of silver at the periphery of the deposit is dramatically illustrated in Figure 2 which shows a SERS map of a number

* To whom all correspondence should be addressed, mmoskovits@ltsc.ucsb.edu.
Received for review: 12/16/2009
Published on Web: 03/01/2010

DOI: 10.1021/nl904173f | *Nano Lett.* **2010,** *10,* 1329–1334

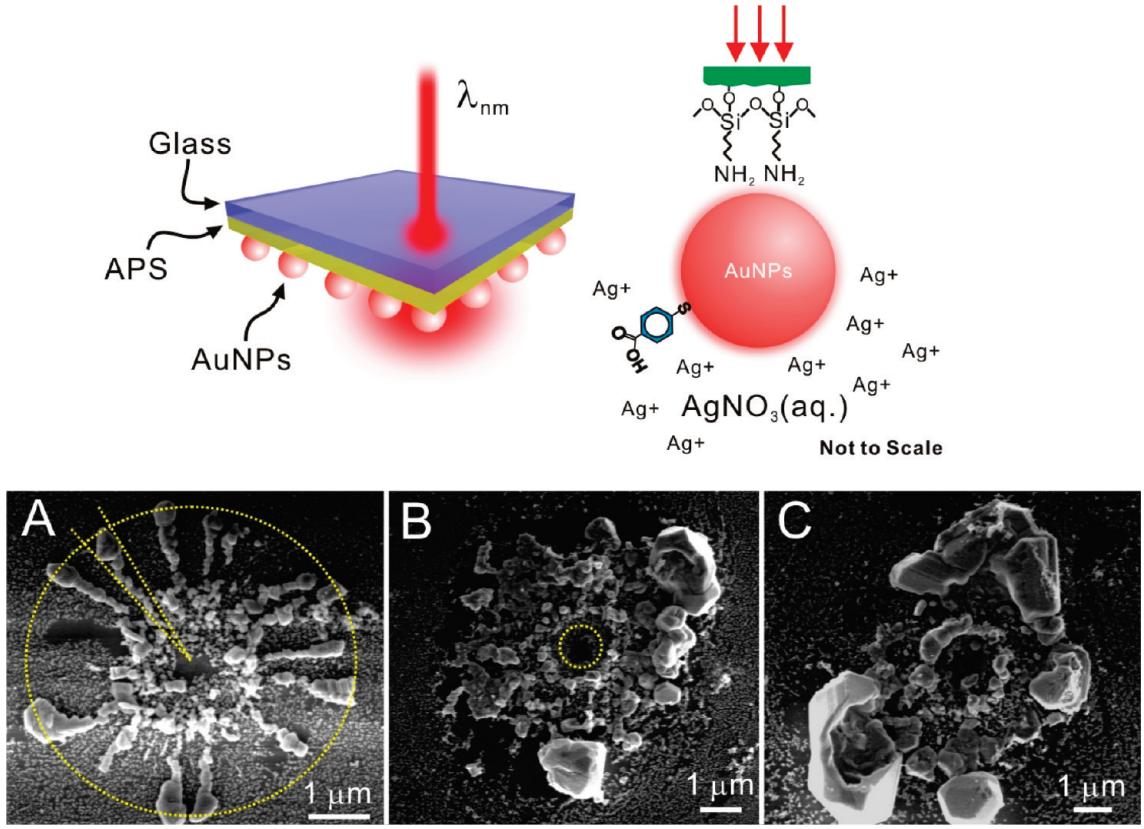

FIGURE 1. (top left) Schematic of the construction of the samples used in the reported experiments. Mercaptobenzoic acid-covered gold nanoparticles are immobilized on (3-aminopropyl)triethoxysilane-functionalized glass in contact with aqueous silver nitrate (details shown schematically top right). (bottom) Scanning electron microscopy images of the Ag deposits resulting from illumination from the glass side of the sample with 4.25 mW of 632.8 nm laser light focused with a 50× objective lens to a ~1 μm spot, after (A) 10 s, (B) 20 s, and (C) 30 s of illumination. The yellow dotted line in A is meant to show that the width of the silver deposit increases approximately proportionally with the radial distance from the center of the deposit. The yellow dotted circle in B corresponds approximately to the size of the focused laser beam.

of silver deposits created by moving the photoreducing laser beam (632.8 nm) sequentially along the surface. Subsequently the sample is exposed to rhodamine 6G and SERS excited with 514.5 nm laser light.

We propose that the symmetrical silver deposits are formed by SP-mediated multiphoton photoemission. The photoemitted electrons reduce silver ions that reside either on the AuNPs and subsequently on the silver particles formed or in the adjacent solution (Figure 1). The photoemitted charge can be captured by the metal and can therefore be conducted to a remote point on the deposit where Ag^+ ion reduction takes place. As structure grows in size beyond the neighborhood of the illuminated spot, reduction would also occur at the periphery of the deposit. And although there are bound to be losses as one conducts the effect of the irradiation outward whatever the propagation mechanism is, that effect would be at least partially compensated for by the increased availability of silver ions as the radius of the deposit grows (Figure 1A), which explains both the flower-like radial symmetry of the silver deposit and the fact that the petals increase in width with increasing radius. Facile electrical conduction only occurs along percolating particles, although less-effective electron propagation can occur through hopping. Additionally, the effect at a distance might also be due to plasmonic conductance.[4] However, the symmetry of the deposits seems less consistent with plasmonic propagation than with one that involved migration of charge.

That surface plasmons are involved is implied by the fact that this process proceeds rapidly with red light illumination (632.8 and 785 nm light produce similar results) but slowly when green light (514.5 nm) is used. The resonance with the SP is much poorer at green wavelengths. By contrast, red light is resonant both with the SP of the isolated Au particles (especially NPs surrounded by a dielectric) and with aggregated silver. With this in mind, the reaction was attempted with AgNPs in place of the AuNPs. With red light no reaction was observed. With green light illumination some silver aggregates were formed but the rate of reaction decreased rapidly with time, consistent with this being a process resonant with the plasmon.[10,11] With red light one has initial resonance with isolated gold nanoparticles and the light continues to be resonant with the resulting aggregated silver product formed. With green light the resonance condition is poor with gold and remains poor for aggregated silver,

DOI: 10.1021/nl904173f | *Nano Lett.* **2010,** *10,* 1329–1334

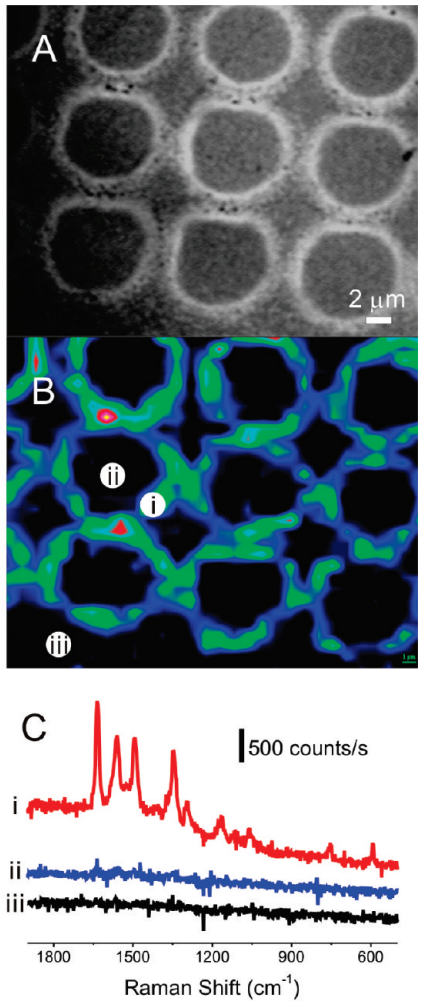

FIGURE 2. (A) Optical microscope image of a series of Ag silver deposits produced by photoreducing Ag ions with 8.5 mW of 632.8 nm laser light as described in Figure 1. Each deposit resulted from 1 s of irradiation. The array shown was produced by repeating the process at 10 μm intervals. (B) SERS map obtained from the deposits shown in (A) after they were washed with water and ethanol, incubated in 1 μM rhodamine 6G solution for 10 min, and then washed again in water and dried at room temperature. SERS spectra were excited with 0.5 mW of 514.5 nm laser light. Spectra were recorded for 1s in 1 μm intervals. The most intense SERS signals are observed at the outer perimeter of the silver deposits where the greatest mass of sliver is deposited. (C) SERS spectra obtained from the locations indicated in panel B.

while with isolated silver nanoparticles resonance with green light is good but resonance is rapidly vitiated as the silver aggregates.

Plasmonically induced photoemission can be accounted for by expressing the SP as a superposition of many excitonic states whose energy of recombination creates hot (i.e., ballistic) electrons, some of which are photoemitted.[12] The fate of the photoelectrons could be multifold: (i) They can combine with adsorbed silver ions to create zerovalent silver atoms that remain on the surface. (ii) They can tunnel into the double layer and there reduce silver ions to silver atoms that are hot as a result of the neutralization energy and diffuse, eventually aggregating to form the growing silver particles (initially by settling on the Au nanoparticles). (iii) They might be transiently captured at the surface of the metal in so-called image states which ultimately react with Ag^+ in solution to form zerovalent silver. In all of these cases silver ions would be replenished by (electric-field assisted) diffusion from the bulk of the electrolyte to the double-layer region near the metal's surface. In all three cases the metal is rendered positive (acting as an oxidizing agent) whose charge neutrality would ultimately need to be restored through the photoelectrochemical oxidation of water or a water-derived species such as hydroxyl or of the nitrate anion which is introduced into solution along with Ag^+. (Full charge neutrality need not strictly be maintained. The positive charge need only be sufficiently neutralized so as to restore the system to a redox state consistent with steady state for the sum of the electrochemical and photoprocesses involved.)

The mechanism proposed above contrasts with that operating in the reaction reported by Maillard et al.,[13] who proposed a plasmon-mediated photo-oxidation reaction of citrate ion to carbon dioxide and a ketonic dicarboxylic acid at the surface of gold nanoparticles (using 457 nm light). The electrons released in the oxidation reaction of the organic species reduce silver ions in solution to zerovalent silver which subsequently aggregates.[14] The reduction of silver upon gold nanoparticles by molecular reducing agents was also used by Mirkin and co-workers[15] and others[16] to enhance SERS activity of their systems. It is also clear that the mechanism operating in producing our deposits contrasts with that taking place in laser-induced silver or gold photodeposition out of, for example, silver nitrate solutions,[17,18] or in silver nitrate-containing polymers[19] which produce very thin conducting lines or other structures for device-wiring applications. In those studies the deposition occurs entirely within the illuminated spot, primarily by a two-photon photoprocess.

That photoemission is the crucial first step was demonstrated as follows. The above experiments were repeated on a slide covered with an ITO conductive layer and the potential was measured during laser irradiation (Figure 3). If, as proposed, photoemission is indeed the first and crucial step, then a positive potential would be measured during irradiation, reflecting the fact that photoemission renders the gold, and subsequently the deposited silver metal, positive. Thus the electron recharge current flowing through a resistor in contact with the ITO would flow from ground to the silver. If oxidation of a molecular species in solution is the first step, then the electrode becomes negative during laser illumination, as was reported for citrate oxidation by Maillard et al.[13]

Figure 3A–C shows the potential responses of the electrode versus time for the system containing Ag+ ions illuminated with 785 nm laser light. The electrode shows positive excursions indicating that the electrode becomes positive, consistent with the first step's being photoemission. No photoresponse was observed, however, when the elec-

DOI: 10.1021/nl904173f | *Nano Lett.* **2010,** *10,* 1329–1334

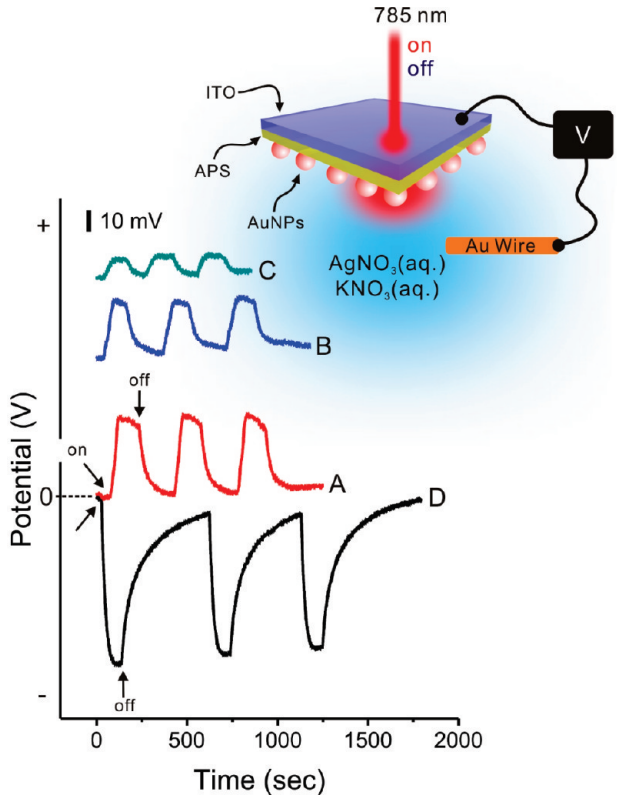

FIGURE 3. (top) Schematic of the sample configuration used in recording the time-dependent potential response to laser illumination. The gold nanoparticles were deposited on (3-aminopropyl)triethoxysilane-functionalized ITO-covered glass (30−60 Ω/sq surface resistivity). Potential measurements were made with respect to a gold counter-electrode immersed in the solution. Prior to these measurements, the electrolyte (KNO_3 (0.1 M) + $AgNO_3$ (1 mM)) was purged with nitrogen gas for ∼15 min to remove oxygen. Time-dependent signals obtained with (A) 185, (B) 90, and (C) 10 mW of 785 nm laser irradiation. (D) Using the experimental configuration employed in carrying out the experiments summarized in curves A−C, we reproduced the experiment reported in ref 13 in which citrate dissolved in the electrolyte is oxidized as a first step. (Using an AgNP-decorated ITO-functionalized surface immersed in aqueous KNO_3 (0.1 M) + citrate (0.5 mM), 250 mW, 514.5 nm.) Note that in curves A−C the electrical current following illumination established a positive voltage at the ITO surface, while for curve D, a negative voltage is observed. The baselines of curves B and C are offset by 0.07 and 0.11 V for clarity.

trolyte was present absent the Ag+ ions. And when citrate was added to the electrolyte, the current excursions became negative (Figure 3D), duplicating the results of Maillard et al.[13] Hence, photoemission appears to be the initiating step that ultimately results in the large-scale reduction and deposition of silver.

If direct reduction of silver ions constitutes the first step, a compensating oxidation reaction needs to occur to (at least partially) restore charge neutrality. Two plausible reactions would be

$$2OH^- \rightarrow HOOH + 2e^-$$

and

$$2H_2O \rightarrow O_2 + 4H^+ + 4e^-$$

There are also several plausible NO_3^- oxidation reactions yielding various combinations of species such as N_2, O_2, NO, NO_2, and, of course, electrons. All of these reactions are higher-energy reactions than the oxidation of citrate and, therefore, not good candidates as initiators of the photoreduction cycle of Ag^+ ions (which citrate can accomplish), but they would eventually take place when the reduction of silver by photoemitted electrons proceeds far enough to raise the electrochemical potential at the metal sufficiently (much as an external positive bias would).

Because it is difficult to measure the mass of the silver deposits directly, the photodynamics of the above process was followed by observing the time evolution of the SERS signal which is significantly more intense for the silver aggregates than for the rather isolated gold nanoparticles. Intense SERS spectra of MBA were found to evolve as a function of 632.8 nm laser irradiation time (Figure 4,A−D). Representative spectra and the time evolution of the 718 cm^{-1} MBA SERS band with time for four laser irradiation powers are shown in Figure 4E. At the lower powers the signal intensity increases monotonically with time and tends toward a saturation value. At the highest powers, the SERS signal declines again at large values of time, undoubtedly reflecting the poorer SERS efficacy of the very large silver particles that form as the reaction proceeds. No MBA was added in these experiments over and above what was already present on the gold. Hence, the signal observed is due to MBA that had been sandwiched between the gold and the deposited silver, plus adsorbate that had diffused from the gold onto the growing silver aggregates, and/or that had desorbed from the gold and readsorbed onto the silver. Adsorbate diffusion would be strongly aided by the increased local temperature that results from the release of the heat of neutralization of the Ag^+ ions—which is a strongly exoergic process (even when correcting for the endoergicity of the release of waters of hydration surrounding Ag^+). Thus the intensity of the spectra might result from more or less the same number of MBA molecules, and therefore the intensity reflects primarily the effect of aggregation, i.e., the multiplication of SERS hot spots, the self-tuning of the aggregates of the excitation wavelength as they grow, and other SERS enhancement processes that aggregation engenders.

The relationship between the SERS intensity and the changing architectural details of the silver deposit is complex with many dynamical and structural parameters that are unknown. We therefore propose the following simplified model consisting of a photochemically induced photoionization first step producing zerovalent silver atoms from silver ions. The rate constant, k_0, associated with this step will be assumed proportional to I^n, where I is the laser intensity and n, the number of photons involved. This is followed by a series of aggregation steps that form small,

DOI: 10.1021/nl904173f | *Nano Lett.* **2010,** *10,* 1329–1334

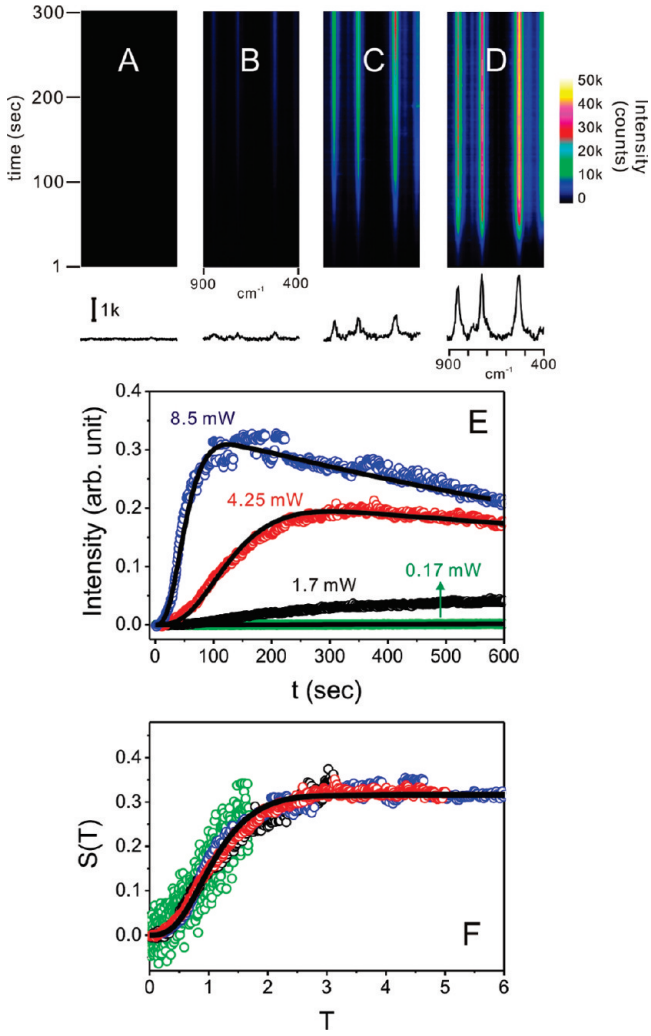

FIGURE 4. (top panel) Time evolution of the SERS spectra following illumination of an MBA/AuNPs/glass sample immersed in 1 mM $AgNO_3$ aqueous solution for four values of the power: (A) 0.17, (B) 1.7, (C) 4.25, and (D) 8.5 mW of 632.8 nm laser light. Spectra were recorded in 1 s intervals, and 1 s data acquisition time. The SERS spectra show signals exclusively from MBA. The initial spectra recorded with 1 s acquisition are shown at the center of the figure, and their evolution over 300 s of laser illumination are shown as false-color streak spectra above them. (E) The evolution of the integrated SERS intensity of the 718 cm^{-1} MBA band versus irradiation time for four values of the laser power. The points are experimental results. Lines are fits to the experimental data using the solutions to eq 1 as described in the Supporting Information. (F) Comparison between the experimental (points) and calculated (lines) early time kinetics for the aggregation dynamics of silver atoms produced from silver ions following two-photon plasmonically mediated photoemission. When plotted against an appropriately scaled dimensionless time, the results are shown to obey a universal curve.

SERS-active silver clusters which we simulate with the first few steps of a stepwise addition reaction. We assume that all of the reaction steps occur close to the metal surface and that silver ion is in excess or at least rapidly replenished by diffusion into the thin reaction zone. Moreover, we will assume that the surface available for the initial photoionization step decreases exponentially with time to account for the irreversible processes occurring in the roughly circular illuminated portion of the surface such as the reduction in the number of gold nanoparticles due to thermally driven particle diffusion out of the illumination zone. (That such reduction occurs is supported by electron microscopic images).

We approximate the silver ion reduction plus subsequent aggregation process by the following simplified scheme

$$\tilde{a}^{+} \rightarrow \tilde{a} \rightarrow \text{small aggregates } (\tilde{s}) \rightarrow \text{large aggregates } (\tilde{l})$$

whose dynamics we approximate by the solution of the following set of simultaneous differential equations

$$\frac{d\tilde{a}}{d\tilde{t}} = k_0 e^{-B\tilde{t}} a^{+} - 2k_1\tilde{a}^2 - k_3\tilde{a}\tilde{s}$$

$$\frac{d\tilde{s}}{d\tilde{t}} = k_1\tilde{a}^2 - 2k_2\tilde{s}^2 - k_3\tilde{a}\tilde{s} \qquad (1)$$

$$\frac{d\tilde{l}}{d\tilde{t}} = k_2\tilde{s}^2 + k_3\tilde{a}\tilde{s}$$

Details of the solution of eq 1 are given in the Supporting Information. The initial surface area of the Au nanoparticles is folded into the value of k_0, while its slow exponential decay is explicitly factored out to allow a proper solution to eq 1. A very good concordance is found between the solution and the observed time evolutions for the SERS intensities recorded with the four values of the laser intensity (Figure 4E). The values of k_0 returned are proportional to I^2 and B is proportional to I. The SERS intensity was assumed to be proportional to the concentration of small aggregates ($\tilde{s}$) in the illuminated area. This implies that the plasmon-mediated photoionization process is biphotonic while the process that depletes the illuminated is a one-photon process. The latter result would make sense if the rate of depletion of the illuminated area of gold nanoparticles is primarily a thermally driven process dependent proportionally on the absorption of the laser light. The validity of the underlying physics approximated by eq 1 is reinforced by the fact that, when appropriately scaled, the "early time" solutions (with time thresholds that advance toward longer times as the laser intensity diminishes) should obey a universal equation independent of the laser intensity (see Supporting Information), which indeed it does (Figure 4F).

The biphotonicity of the photoemission process requires some discussion. The work functions of gold and silver are, ~4.8 and ~4.7 eV, respectively. Accordingly, it would take three photons with vacuum wavelengths of 632.8 and 785 nm (1.96 and 1.57 eV, respectively) to clear the ionization threshold of gold or silver in vacuum. In an aqueous medium, however, the energy requirements are less stringent as is well-known from photography and other photoreduc-

DOI: 10.1021/nl904173f | *Nano Lett.* **2010,** *10,* 1329–1334

tive studies of silver nitrate such as the aforementioned two-photon silver reduction processes.[15,16] Moreover, one can visualize lower-energy processes that could lead to electron migration along the percolating metal. For example, a conduction electron could quantum tunnel and become trapped in an image state of the metal's surface.[20] Because of the stability of the electron in the image state, the energy requirements of such a process are significantly lower than the 4.7 eV needed to clear the workfunction of the metal. Once created, the image-bound electrons can migrate across the surface rather freely. What our results imply is that in the photoprocess occurring in our system clearing the photoemission barrier seems to be the rate-determining step.

A rough value for the quantum efficiency of the above process was obtained by estimating the mass of deposited silver observed by scanning electron microscopy, and referencing the equivalent number of silver atoms to the number of photons illuminating that spot. The value obtained, $\sim 1 \times 10^{-5}$, is not inconsistent with a two-photon process.

The dependence on laser fluence was also determined from the photoemission current directly. As expected, the results show rather rapid saturation (Figure 3A−C) suggesting that the excitation of the SP is a facile process leading to rapid positive charge buildup (as reflected by the direct measurements) so that as the laser fluence is increased the residual positive charge left behind on the electrode impedes further photoemission, rapidly establishing a steady state in which the dependence of the recharge current on laser fluence is approximately linear.

In summary, when exposed to red light, surface-immobilized gold nanoparticles in contact with aqueous silver ions rapidly photoreduce the silver ions producing radially symmetric metal deposits with diameters many times larger than the diameter of the illuminating laser beam. We propose that this reduction-at-a-distance effect arises from two-photon, surface-plasmon-mediated photoemission with the resulting electrons conducting along percolating silver pathways reducing silver ions along the way and at their periphery increasing thereby the size of the deposit far beyond illuminated area (and perhaps assisted by plasmonic conductance along the "nanowires" formed leading to remote photoionization). SERS measurements from the growing silver deposits suggest that the process is biphotonic.

Acknowledgment. This work was supported by the Institute for Collaborative Biotechnologies through Grant DAAD19-03-D- 0004 from the U.S. Army Research Office and made extensive use of the MRL Central Facilities at UCSB supported by the National Science Foundation under Award Numbers DMR-0080034 and DMR-0216466 for the HRTEM/STEM microscopy. We also gratefully acknowledge research support from the Institute for Energy Efficiency, an Energy Frontier Research Center funded by the U.S. Department of Energy, Office of Science, Office of Basic Energy Sciences, Award Number: DE-SC0001009.

Supporting Information Available. Description of experimental data fit including two additional figures. This material is available free of charge via the Internet at http://pubs.acs.org.

REFERENCES AND NOTES

(1) Moskovits, M. *Rev. Mod. Phys.* **1985**, *57*, 783–826.
(2) Prodan, E. M.; Radloff, C.; Halas, N. J.; Nordlander, P. *Science* **2003**, *302*, 419–422.
(3) Garcia-Vidal, F. J.; Pendry, J. B. *Phys. Rev. Lett.* **1996**, *77*, 1163–1166.
(4) Barnes, W. L.; Dereux, A.; Ebbesen, T. W. *Nature* **2003**, *424*, 824–830.
(5) Nitzan, A.; Brus, L. E. *J. Chem. Phys.* **1981**, *75*, 2205.
(6) Goncher, G. M.; Harris, C. B. *J. Chem. Phys.* **1982**, *77*, 3767–3768.
(7) Wolkow, R. A.; Moskovits, M. *J. Chem. Phys.* **1987**, *87*, 5858–5869.
(8) Kamisetty, N. K.; Pack, S. P.; Nonogawa, M.; Devarayapalli, K. C.; Kodaki, T.; Makino, K. *Chem. Lett.* **2007**, *36*, 322–323.
(9) Grabar, K. C.; Freeman, R. G.; Hommer, M. B.; Natan, M. J. *Anal. Chem.* **1995**, *67*, 735–743.
(10) Cañamares, M. V.; Garcia-Ramos, J. V.; Gómez-Varga, J. D.; Domingo, C.; Sanchez-Cortes, S. *Langmuir* **2007**, *23*, 5210–5215.
(11) Zheng, X.; Xu, W.; Corredor, C.; Xu, S.; An, J.; Zhao, B.; Lombardi, J. R. *J. Phys. Chem. C* **2007**, *111*, 14962–14967.
(12) Stuckless, J. T.; Moskovits, M. *Phys. Rev. B* **1989**, *40*, 9997–9998.
(13) Maillard, M.; Huang, P.; Brus, L. *Nano Lett.* **2003**, *3*, 1611–1615.
(14) Redmond, P. L.; Wu, X.; Brus, L. *J. Phys. Chem. C* **2007**, *111*, 8942–8947.
(15) Cao, Y. C.; Jin, R.; Mirkin, C. A. *Science* **2002**, *297*, 1536–1540.
(16) Sun, L.; Yu, C.; Irudayaraj, J. *Anal. Chem.* **2008**, *80*, 3342–3349.
(17) Tanaka, T.; Ishikawa, A.; Kawata, S. *Appl. Phys. Lett.* **2006**, *88*, No. 081107.
(18) Bjerneld, E. J.; Svedberg, F.; Käll, M. *Nano Lett.* **2003**, *3*, 593–596.
(19) Maruo, S.; Saeki, T. *Opt. Express* **2008**, *16*, 1174–1179.
(20) Harris, C. B.; Ge, N.-H.; Lingle, R. L.; McNeill, J. D., Jr.; Wong, C. M. *Annu. Rev. Phys. Chem.* **1997**, *48*, 711–744.

DOI: 10.1021/nl904173f | *Nano Lett.* **2010,** *10,* 1329–1334